Refractive index sensors based on the fused tapered special multi-mode fiber*

FU Xing-hu (付兴虎)[1,2]**, **XIU Yan-li** (修艳丽)[1], **LIU Qin** (刘琴)[1], **XIE Hai-yang** (谢海洋)[1], **YANG Chuan-qing** (杨传庆)[1], **ZHANG Shun-yang** (张顺杨)[1], **FU Guang-wei** (付广伟)[1,2], and **BI Wei-hong** (毕卫红)[1,2]

1. School of Information Science and Engineering, Yanshan University, Qinhuangdao 066004, China

2. The Key Laboratory for Special Fiber and Fiber Sensor of Hebei Province, Qinhuangdao 066004, China

(Received 23 August 2015)

In this paper, a novel refractive index (RI) sensor is proposed based on the fused tapered special multi-mode fiber (SMMF). Firstly, a section of SMMF is spliced between two single-mode fibers (SMFs). Then, the SMMF is processed by a fused tapering machine, and a tapered fiber structure is fabricated. Finally, a fused tapered SMMF sensor is obtained for measuring external RI. The RI sensing mechanism of tapered SMMF sensor is analyzed in detail. For different fused tapering lengths, the experimental results show that the RI sensitivity can be up to 444.517 81 nm/RIU in the RI range of 1.334 9—1.347 0. The RI sensitivity is increased with the increase of fused tapering length. Moreover, it has many advantages, including high sensitivity, compact structure, fast response and wide application range. So it can be used to measure the solution concentration in the fields of biochemistry, health care and food processing.

Document code: A **Article ID:** 1673-1905(2016)01-0012-4

DOI 10.1007/s11801-016-5160-0

Optical fiber refractive index (RI) sensor[1,2] is very important in biology, chemistry and medicine fields due to the advantages of high sensitivity, compact size and fast response. It has several kinds of common structures, including the core offset splicing[3,4], material coating[5,6], fiber grating[7,8] and so on. For example, Shan Zhu et al[9] introduced the atomic layer deposition technology to fabricate a high sensitivity RI sensor based on an adiabatic tapered optical fiber, where an asymmetric Fabry-Perot like interferometer is constructed along the fiber taper. Peter Tatar et al[10] proposed a modification structure model of in-fiber sensor based on intermodal interference in two core photonic crystal fibers for measuring external RI. Especially, an increase of RI sensitivity to the surrounding medium could be achieved by decreasing the fiber diameter. It is the most common solution to etching the fiber cladding with chemical reagent. However, this method has the disadvantages of low control precision and large repeatability error. So the fused tapered method is proposed and applied in different fiber sensor, mainly including the flame brushing technique and CO_2 laser fusion technology. For example, Le Xu et al[11] proposed a high-temperature sensor based on an abrupt fiber-taper Michelson interferometer in single-mode fiber (SMF) fabricated by a fiber-taper machine and electric-arc discharge, S. A. Ibrahim et al[12] proposed an ammonia sensor composed of a tapered multimode fiber coated with polyaniline nanofibers, and Fu Guangwei et al[13] analyzed an RI sensor of photonic crystal fiber Mach-Zehnder interferometer (MZI) based on CO_2 laser fusion technology. Due to the controllable accuracy and simple preparation of fused tapered method, an RI sensor is proposed based on the fused tapered special multi-mode fiber (SMMF).

In this paper, an RI sensor is fabricated by using a section of SMMF, which is spliced between two SMFs, and then tapered down by flame brushing technique. The RI sensing principle is analyzed, and the testing experiments are performed. By changing the tapering length of SMMF, three RI sensors are fabricated and characterized in detail. Then these experimental results are analyzed and discussed. In the RI range of 1.334 9—1.347 0, this sensor has good RI sensitivity.

The cross section of the SMMF used in our experiment is shown in Fig.1. It is composed by pure silica core and glass cladding, which is fabricated by Yangtze Optical Fiber and Cable Joint Stock Limited Company. It is a step-index fiber with a standard 105/125 μm structure size.

Typically, the RI sensor consists of an SMMF section spliced between two SMFs, forming an SMF-SMMF-SMF structure. Then the SMMF is processed by a fused tapering machine (SCS-4000), and a tapered fiber struc-

* This work has been supported by the National Natural Science Foundation of China (Nos.61205068 and 61475133), the Hebei Province Science and Technology Support Program (Nos.15273304D and 14273301D), the College Youth Talent Project of Hebei Province (No.BJ2014057), the "XinRuiGongCheng" Talent Project and the Excellent Youth Funds for School of Information Science and Engineering in Yanshan University (No.2014201).

** E-mail: fuxinghu@ysu.edu.cn

ture is fabricated. So we can obtain a fused tapered SMMF sensor for measuring external RI as shown in Fig.2.

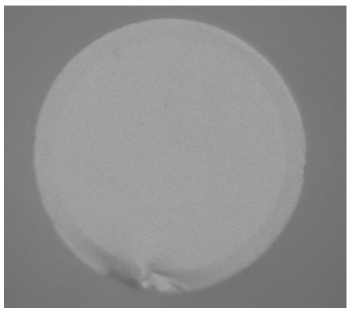

Fig.1 The cross section of SMMF

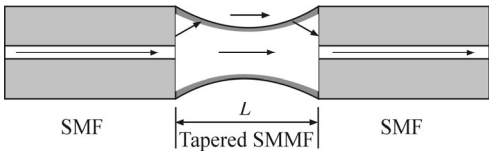

Fig.2 Schematic diagram of the fused tapered SMMF sensor

In Fig.2, we can see that the tapered SMMF is connected between two SMFs. In general, the light in the SMMF is transmitted in core, but the fiber core and cladding diameters become thinner due to the fused tapered procedure, so the light in core can be transmitted along with the surface of the tapered SMMF due to the evanescent wave. Therefore, a miniature MZI is realized, and the sensing principle is as follows.

The tapered sensing area L is the region outside the tapered SMMF core. Light from the input SMF through the first fusion junction, a part of light energy is coupled into the tapered SMMF core as the reference arm, and the other part of light energy is coupled into the tapered sensing area as the signal arm. As the tapered SMMF gradually becomes thinner, the core mode is coupled to the cladding mode gradually, and the optical energy transmitted in the core mode is gradually weakened, while the light energy transmitted in the tapered sensing area is gradually enhanced. When the two parts are propagated to the second fusion junction, the cladding mode of the tapered sensing area and the core mode transmitted in the tapered SMMF core are interfered in the output SMF. Therefore, based on the theory of optical fiber MZI, the influence mechanism of tapered SMMF sensor is studied.

In the MZI based on the tapered SMMF sensor, the intensity and the center wavelength[14] of the interference spectrum can be expressed as

$$I = I_1 + I_2 + 2\sqrt{I_1 I_2}\cos\left(2\pi n_{\text{cor-cla}} L/\lambda\right), \tag{1}$$

$$\lambda_m = \frac{n_{\text{cor-cla}} L}{m}, \tag{2}$$

where I is total output light intensity, I_1 and I_2 is the light intensity in fiber core and tapered sensing area, respectively, λ_m is the central wavelength of mth order interference fringe, L is the interference length, i.e., the distance of tapered sensing area, and $n_{\text{cor-cla}}$ is the difference between the core RI and the effective RI of tapered sensing region.

The wavelength shift caused by the change of RI in tapered sensing area can be expressed as

$$\Delta\lambda_m = \frac{(n_{\text{cor-cla}} + \Delta n_{\text{cor-cla}})L}{m} - \frac{n_{\text{cor-cla}} L}{m} = \frac{\Delta n_{\text{cor-cla}} L}{m}, \tag{3}$$

where $\Delta\lambda_m$ is the center wavelength shift for the mth order interference fringe, $\Delta n_{\text{cor-cla}}$ is the variation of RI difference caused by the RI changing in tapered sensing area.

With the environmental RI changing, $\Delta n_{\text{cor-cla}}$ will also change. It leads to the variation of phase difference between fiber core mode and cladding mode, and the interference fringe will also shift. Thereby, the external RI can be detected by measuring the interference fringe shift.

In order to investigate the RI sensing characteristics, a straight experiment is performed with experimental setup as shown in Fig.3.

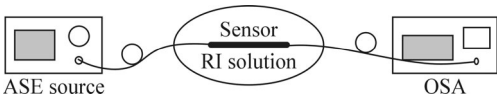

Fig.3 Experimental setup for RI measurement

In Fig.2, an amplified spontaneous emission (ASE) optical source is used for measuring, whose wavelength ranges from 1 520 nm to 1 610 nm. An optical spectrum analyzer (OSA, YOKOGAWA AQ6375) is used to record the spectrum with different RIs.

During the whole experiment, the proposed fused tapered SMMF sensor is placed in glassware. The interference spectra are recorded and analyzed experimentally in RI range of 1.334 9—1.347 0. Based on Eq.(3), different tapered sensing area lengths can cause the variation of center wavelength shift. Thereby, three sensors with different sensing area lengths are taken as examples for measuring RI.

When the SMMF initial length is 30 mm and the fused tapering length is 8 mm, the interference spectra of the first sensor with different RIs of 1.334 9, 1.336 6, 1.338 5, 1.340 2, 1.342 0, 1.343 5, 1.345 9 and 1.347 0 are shown in Fig.4.

In Fig.4, we can see that the interference spectrum has obvious shift towards long wavelength with the increase of RI. In order to descript the changes of the interference spectra with different RIs in detail, the extreme wavelengths near 1 533 nm in spectra are selected as the observation points. The relationship between RI and wavelength shift is shown in Fig.5. As shown in Fig.5, it

shows that the tapered SMMF sensor has high RI sensitivity of 209.312 83 nm/RIU.

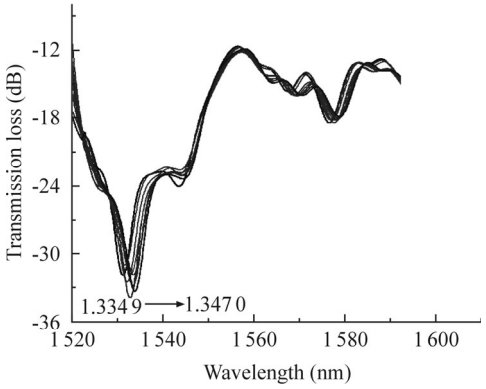

Fig.4 Interference spectra of the first sensor corresponding to different RIs

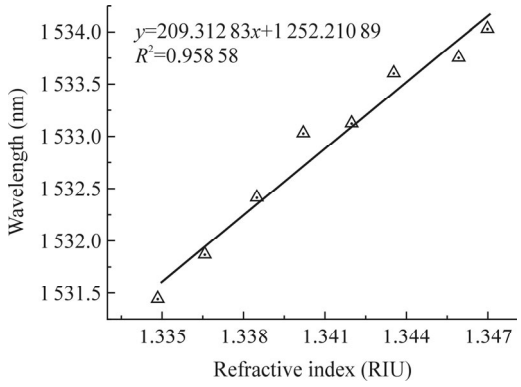

Fig.5 Relationship between RI and wavelength shift for the first sensor

When the SMMF initial length is 30 mm, and the fused tapering lengths are 12 mm and 15 mm, respectively, the interference spectra of other two sensors with different RIs are shown in Figs.6 and 7.

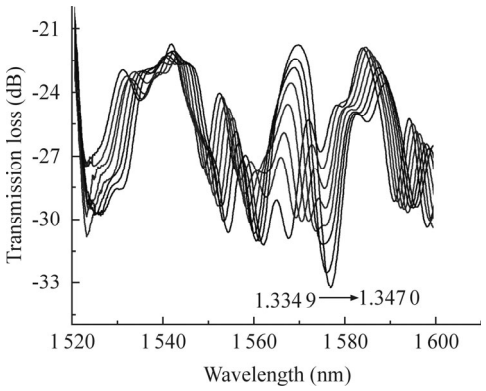

Fig.6 Interference spectra of the second sensor corresponding to different RIs

Similarly, we can see that with the increase of RI, the interference spectrum has obvious shift towards long wavelength in Figs.6 and 7. The extreme wavelengths near 1 595 nm in the spectra are selected as the observation points in Fig.6, and the extreme wavelengths near 1 585 nm in the spectra are selected in Fig.7, respectively. So we can obtain the relationships between RI and wavelength shift for the second and the third sensors as shown in Figs.8 and 9.

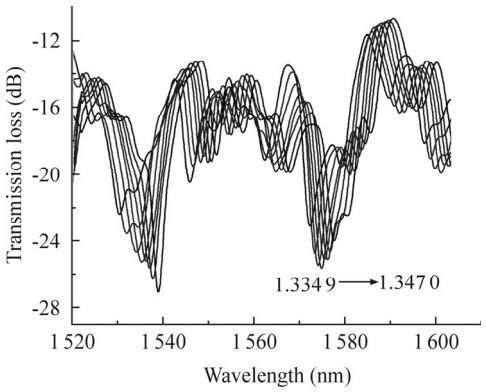

Fig.7 Interference spectra of the third sensor corresponding to different RIs

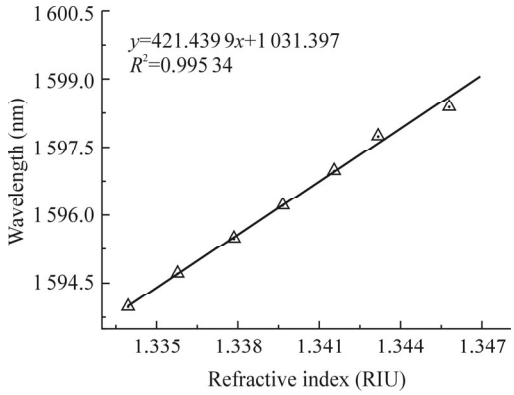

Fig.8 Relationship between RI and wavelength shift for the second sensor

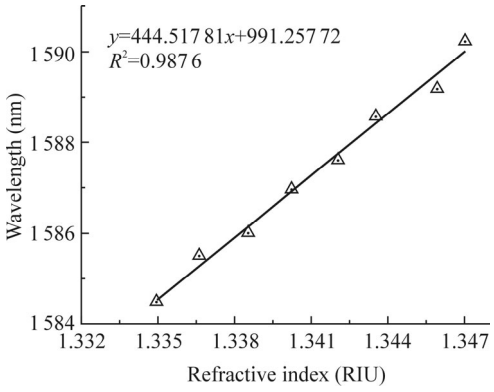

Fig.9 Relationship between RI and wavelength shift for the third sensor

In Figs.8 and 9, the second and the third tapered SMMF sensors have high RI sensitivities of 421.439 9 nm/RIU and 444.517 81 nm/RIU, respectively. So these three sensors have perfect RI sensing performances. Moreover, in the

RI range of 1.334 9—1.347 0, the longer the tapering length of the sensor is, and the higher the RI sensitivity is. That is mainly because the tapered sensing area lengths are different. For a certain mth order interference fringe, the center wavelength shift $\Delta\lambda_m$ is increased when $\Delta n_{\text{cor-cla}}$ is the same. Thereby, the variation of external RI can be determined by measuring the wavelength shift of observation point.

A novel RI sensor based on the fused tapered SMMF is described. The RI sensing mechanism of the tapered SMMF sensor is analyzed in detail, and a demonstrated set up is performed experimentally. Experimental results show that the RI sensing sensitivity can be up to 444.517 81 nm/RIU in the RI range of 1.334 9—1.347 0. The RI sensitivity is increased with the increase of fused tapering length. Moreover, it has many advantages including high sensitivity, compact structure, fast response and wide application range. So it can be used to measure the solution concentration in the fields of biochemistry, health care and food processing.

References

[1] Wen Xiaodong, Ning Tigang, You Haidong, Li Jing, Feng Ting, Pei Li and Jian Wei, Optoelectronics Letters **9**, 325 (2013).

[2] Hongyun Meng, Wei Shen, Guanbin Zhang, Xiaowei Wu, Wei Wang, Chunhua Tan and Xuguang Huang, Sensors and Actuators B: Chemical **160**, 720 (2011).

[3] Xinpu Zhang, Wei Peng, Yun Liu and Lujun Pan, Optics Communications **294**, 188 (2013).

[4] Cheng Huaqi, Jing Zhenguo, Peng Wei, Hao Huali, Li Hong and Zhang Xinpu, Journal of Optoelectronics·Laser **26**, 649 (2012). (in Chinese)

[5] Ying Zhao, Fufei Pang, Yanhua Dong, Jianxiang Wen, Zhenyi Chen and Tingyun Wang, Optics Express **21**, 26136 (2013).

[6] Gan Huanbiao, Chen Zhe, Zhang Jun, Gan Hongbo，Tang Jieyuan, Luo Yunhan, Yu Jianhui, Lu Huihui and Guan Heyuan, Journal of Optoelectronics·Laser **26**, 633 (2015). (in Chinese)

[7] Cao Ye, Liu Huiying, Tong Zhengrong, Yuan Shuo and Zhao Shun, Optoelectronics Letters **11**, 69 (2015).

[8] Shi Shenghui, Zhou Xiaojun, Zhang Zhiyao and Liu Yong, Journal of Optoelectronics·Laser **23**, 1644 (2012). (in Chinese)

[9] Shan Zhu, Fufei Pang, Sujuan Huang, Fang Zou, Yanhua Dong and Tingyun Wang, Optics Express **23**, 13880 (2015).

[10] Peter Tatar and Daniel Kacik, Optical Fiber Technology **19**, 330 (2013).

[11] Le Xu, Lan Jiang, Sumei Wang, Benye Li and Yongfeng Lu, Applied Optics **52**, 2038 (2013).

[12] S. A. Ibrahim, N. A. Rahman, M. H. Abu Bakar, S. H. Girei, M. H. Yaacob, H. Ahmad and M. A. Mahdi, Optics Express **23**, 2837 (2015).

[13] Fu Guangwei, Guo Peng, Fu Xinghu, Bi Weihong and Gao Feilong, Journal of Optoelectronics·Laser **25**, 1657 (2014). (in Chinese)

[14] Ji Yushen, Fu Guangwei, Fu Xinghu, Shen Yuan and Bi Weihong, Acta Optica Sinica **33**,1006005 (2013). (in Chinese)